Chemistry of Polynuclear Metal Complexes with Bridging Carbene or Carbyne Ligands. Part 84.[1] Carbaborane Tungsten–Platinum Complexes having a μ-CC$_6$H$_3$Me$_2$-2,6 Ligand; Crystal Structures of [WPt(μ-CC$_6$H$_3$Me$_2$-2,6)(CO)$_n$(PEt$_3$)(μ-σ:η^5-C$_2$B$_9$H$_8$Me$_2$)] (n = 2 or 3) *

David D. Devore, Judith A. K. Howard, John C. Jeffery, Massimino U. Pilotti, and F. Gordon A. Stone
Department of Inorganic Chemistry, The University, Bristol BS8 1TS

The reaction between the salts [PtH(Me$_2$CO)(PEt$_3$)$_2$][BF$_4$] and [NEt$_4$][W($\equiv$CC$_6$H$_3$Me$_2$-2,6)(CO)$_2$(η^5-C$_2$B$_9$H$_9$Me$_2$)] in acetone at low temperature (*ca.* −30 °C) affords the dimetal compound [WPtH(μ-CC$_6$H$_3$Me$_2$-2,6)(CO)$_2$(PEt$_3$)(η^5-C$_2$B$_9$H$_9$Me$_2$)], in which the carbaborane ligand forms a B–H$\rightharpoonup$Pt three-centre bond by employing a BH group in the pentagonal face of the cage. This product readily affords, *via* loss of hydrogen, the complex [WPt(μ-CC$_6$H$_3$Me$_2$-2,6)(CO)$_2$(PEt$_3$)(μ-σ:η^5-C$_2$B$_9$H$_8$Me$_2$)] as a mixture of two isomers. The structure of the major isomer (*ca.* 80%) has been established by *X*-ray diffraction. The W–Pt bond [2.728(1) Å] is asymmetrically bridged by the CC$_6$H$_3$Me$_2$-2,6 group [μ-C–W 1.88(2), μ-C–Pt 2.15(2) Å]. Indeed with a W–μ-C–C^1(C$_6$H$_3$) angle of 175(1)° these three atoms are nearly linear. The carbaborane ligand has undergone 'slippage' along the W–Pt vector to accommodate formation of a direct exopolyhedral B–Pt σ bond [2.01(2) Å]. This linkage involves the central boron in the $\overline{\mathrm{C{-}C{-}B{-}}\mathit{B}\mathrm{{-}B}}$ face of the icosahedral fragment η^5 bonded to tungsten. The PEt$_3$ ligand attached to the platinum atom [Pt–P, 2.251(7) Å] is transoid to the μ-C and W atoms [μ-C–Pt–P, 160.6(4)°, W–Pt–P 155.9(1)°]. The n.m.r. data (^{1}H, ^{13}C-{^{1}H}, ^{11}B-{^{1}H}, and ^{31}P-{^{1}H}) are in accord with the structure established by the *X*-ray diffraction study. Similar data for the minor isomer reveal that this species had a structure in which the B–Pt σ bond involves a boron atom $\overline{\mathrm{C{-}C{-}}\mathit{B}\mathrm{{-}B{-}B}}$ in the face of the cage, adjacent to a CMe group. The two isomers may be separated by column chromatography, but solutions equilibrate on standing. Formation of the major isomer from [WPtH(μ-CC$_6$H$_3$Me$_2$-2,6)(CO)$_2$(PEt$_3$)(η^5-C$_2$B$_9$H$_9$Me$_2$)] can be partially reversed by treating solutions of the former with hydrogen. Mechanisms are proposed for these various transformations based in part on deuteriation studies employing [PtD(Me$_2$CO)(PEt$_3$)$_2$][BF$_4$] as a precursor to the W–Pt species. The compound [WPt(μ-CC$_6$H$_3$Me$_2$-2,6)(CO)$_2$(PEt$_3$)(μ-σ:η^5-C$_2$B$_9$H$_8$Me$_2$)] (major isomer) is relatively inert to the addition of ligands at the formally 14-electron platinum centre, presumably due to the presence of the bulky xylyl group. However, reactions very readily occur with rod-like ligands (L = CO or CNBu^t) to give the compounds [WPt(μ-CC$_6$H$_3$Me$_2$-2,6)(CO)$_2$(PEt$_3$)(L)(μ-σ:η^5-C$_2$B$_9$H$_8$Me$_2$)]. Indeed the tricarbonyl complex is a major constituent of the mixture of products obtained by treating the complex [NEt$_4$][W($\equiv$CC$_6$H$_3$Me$_2$-2,6)(CO)$_2$(η^5-C$_2$B$_9$H$_9$Me$_2$)] with [PtH(Me$_2$CO)(PEt$_3$)$_2$][BF$_4$]. An *X*-ray study of the carbon monoxide adduct revealed a structure similar to the precursor with parameters W–Pt, 2.728(1), μ-C–W 1.89(1), μ-C–Pt 2.29(1), B–Pt 2.16(1) Å, W–μ-C–C^1(C$_6$H$_3$) 160.0(8), and P–Pt–W 138.5(1)°. The significantly lower W–μ-C–C^1(C$_6$H$_3$) angle (*ca.* 160°) compared with that in the precursor is presumably a consequence of the presence of the additional CO ligand terminally bound to the platinum and cisoid to the alkylidyne group [μ-C–Pt–CO 83.5(4)°].

We have recently described a novel reaction between the two salts [PtH(Me$_2$CO)(PEt$_3$)$_2$][BF$_4$] and [N(PPh$_3$)$_2$][W($\equiv$CC$_6$H$_4$Me-4)(CO)$_2$(η^5-C$_2$B$_9$H$_9$Me$_2$)] (**1a**),[2] which affords the dimetal compound [WPt(CO)$_2$(PEt$_3$)$_2${η^6-C$_2$B$_9$H$_8$(CH$_2$C$_6$H$_4$Me-4)Me$_2$}] (**2**). The latter has a very short metal–metal distance [2.602(1) Å], as might be expected for a double bond, and the carbaborane ligand is η^6 co-ordinated to the tungsten *via* six atoms $\overline{\mathrm{B{-}C{-}B{-}B{-}B{-}C}}$ of the cage. However, the pentahapto bonding of the carbaborane group is restored upon treatment of (**2**) with PMe$_3$, when the complex [WPt(μ-H)(CO)$_2$(PMe$_3$)(PEt$_3$)$_2${μ-σ:η^5-C$_2$B$_9$H$_7$(CH$_2$C$_6$H$_4$Me-4)Me$_2$}] (**3**) is formed. The reactions leading first to (**2**) and then to (**3**) represent in metallacarbaborane chemistry an unprecedented sequence of *closo* to *isocloso* (or *hypercloso*) to *closo* transformations of a C$_2$B$_9$W 12-vertex framework.[3] Moreover, in the synthesis of (**2**) the *p*-tolylmethylidyne ligand present in the precursor (**1a**) migrates to the cage, and in this process is converted to a BCH$_2$C$_6$H$_4$Me-4 group. As discussed earlier,[2] it is possible that the latter is formed *via* an intermediate in which the W–Pt bond is bridged both by an alkylidene fragment μ-CH(C$_6$H$_4$Me-4) and a B–H$\rightharpoonup$Pt three-centre two-electron bond involving the central boron atom of the pentagonal face of the icosahedral η^5-C$_2$B$_9$H$_9$Me$_2$ ligand. Insertion of the μ-alkylidene group into the B–H bond activated *via* ligation to platinum, would then provide a route to the final product.

In an attempt to increase our understanding of the reaction

---

* 2,2-Dicarbonyl and 1,2,2-tricarbonyl-μ-(2,6-dimethyltolylmethylidyne)-μ-[σ:7′—11′-η-octahydro-7′,8′-dimethyl-7′,8′-dicarba-*nido*-undecaborato(3−)-$C^{7',8'}$,$B^{9'-11'}$(W), $B^{10'}$(Pt)]-1-(triethylphosphine)-platinumtungsten (*Pt–W*) respectively.

Supplementary data available: see Instructions for Authors, *J. Chem. Soc., Dalton Trans.*, 1989, Issue 1, pp. xvii—xx.

Table 1. Hydrogen-1 and carbon-13 n.m.r. data[a] for the tungsten–platinum compounds

Compound	$^1H(\delta)$[b,c]	$^{13}C(\delta)$[d]
(**4**)	−10.22 [br, 1 H, PtH, *J*(PtH) 1 165], −4.7 [br, 1 H, B(μ-H)Pt], 0.97 [d of t, 9 H, $P(CH_2Me)_3$, *J*(HH) 7, *J*(PH) 18], 1.95 [m, 6 H, $P(CH_2Me)_3$], 2.23 (s, 6 H, CMe or Me_2-2,6), 2.43 (s, 6 H, CMe or Me_2-2,6), 7.04 (m br, 3 H, C_6H_3)	[e]277.2 [d, μ-C, *J*(PC) 29], 221.4 (WCO), 157.4 [$C^1(C_6H_3)$], 134.8 (C_6H_3), 62.9 (CMe), 30.4 (CMe), 22.7 (Me_2-2,6), 21.7 [d, $P(CH_2Me)_3$, *J*(PC) 38], 8.9 [$P(CH_2Me)_3$]
(**5a**)	0.76 [d of t, 9 H, $P(CH_2Me)_3$, *J*(HH) 8, *J*(PH) 18], 1.57 [m, 6 H, $P(CH_2Me)_3$], 2.16 (s, 6 H, CMe or Me_2-2,6), 2.42 (s, 6 H, CMe or Me_2-2,6), 7.08, 7.33 [AB_2, 3 H, C_6H_3, *J*(AB) 8]	279.9 [d, μ-C, *J*(PC) 22, *J*(WC) 146], 222.5 (WCO), 143.0 140.7, 131.9, 127.8 (C_6H_3), 58.7 (CMe), 30.1 (CMe), 21.7 (Me_2-2,6), 19.4 [d, $P(CH_2Me)_3$, *J*(PC) 29], 9.0 [$P(CH_2Me)_3$]
(**5b**)	0.82 [d of t, 9 H, $P(CH_2Me)_3$, *J*(HH) 8, *J*(PH) 18], 1.71 [m, 6 H, $P(CH_2Me)_3$], 2.15, 2.55 (s × 2, 6 H, CMe), 2.40 (s, 6 H, Me_2-2,6), 7.10, 7.36 [AB_2, 3 H, C_6H_3, *J*(AB) 7]	273.7 [d, μ-C, *J*(PC) 24], 221.2, 218.6 (WCO), 143.6, 139.7, 132.2, 128.2 (C_6H_3), 62.5, 57.3 (CMe), 36.1, 29.9 (CMe), 21.5 (Me_2-2,6), 19.0 [d, $P(CH_2Me)_3$, *J*(PC) 34], 8.8 [$P(CH_2Me)_3$]
(**6a**)	0.99 [d, of t, 9 H, $P(CH_2Me)_3$, *J*(HH) 7, *J*(PH) 18], 2.14 [m, 6 H, $P(CH_2Me)_3$], 2.25 (s, 6 H, CMe or Me_2-2,6), 2.41 (s, 6 H, CMe or Me_2-2,6), 6.99, 7.11 [AB_2, 3 H, C_6H_3, *J*(AB) 7]	287.9 [d, μ-C, *J*(PC) 29], 221.5 (WCO), 214.5 [d, PtCO, *J*(PC) 19], 155.4 [$C^1(C_6H_3)$], 133.8, 127.8, 127.7 (C_6H_3), 62.1 (CMe), 30.8 (CMe), 22.0 (Me_2-2,6), 19.0 [d, $P(CH_2Me)_3$, *J*(PC) 38, *J*(PtC) 38], 8.7 [$P(CH_2Me)_3$, *J*(PtC) 28]
(**6b**)	0.98 [d of t, 9 H, $P(CH_2Me)_3$, *J*(HH) 8, *J*(PH) 17], 1.11 (s, 9 H, Bu^t), 2.07 [m, 6 H, $P(CH_2Me)_3$], 2.23 (s, 6 H, CMe or Me_2-2,6), 2.28 (s, 6 H, CMe or Me_2-2,6), 6.95, 7.08 [AB_2, 3 H, C_6H_3, *J*(AB) 7]	291.7 [d, μ-C, *J*(PC) 38], 224.0 [WCO, *J*(WC) 174], 157.5 [$C^1(C_6H_3)$], 132.7, 127.5 (C_6H_3), 127.3 ($CNBu^t$), 126.4 (C_6H_3), 60.9 (CMe), 58.5 ($CNCMe_3$), 30.8 (CMe), 29.4 ($CNCMe_3$), 21.8 (Me_2-2,6), 18.6 [d, $P(CH_2Me)_3$, *J*(PC) 36, *J*(PtC) 36], 8.8 [$P(CH_2Me)_3$, *J*(PtC) 25]

[a] Chemical shifts (δ) in p.p.m., coupling constants in Hz, measurements at room temperature. [b] Measured in CD_2Cl_2. [c] Proton resonances for BH groups occur as broad unresolved signals in the range δ 0—3 p.p.m. [d] Hydrogen-1 decoupled, chemical shifts are positive to high frequency of $SiMe_4$, with measurements in CD_2Cl_2–CH_2Cl_2 unless otherwise stated. [e] In C_6D_6, resulting in some signals of C_6H_3 group not being observed.

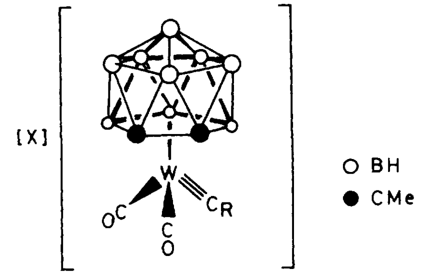

	X	R
(**1a**)	$N(PPh_3)_2$	C_6H_4Me-4
(**1b**)	NEt_4	$C_6H_3Me_2$-2,6

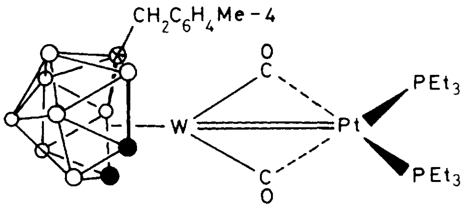

(**2**) ● CMe O BH ⊕ B

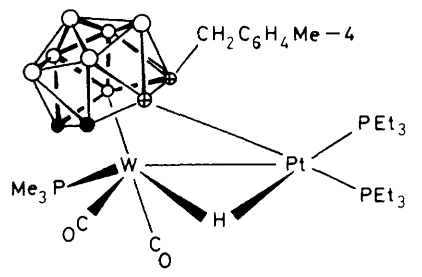

(**3**)

pathways leading to (**2**) and (**3**), and related tungsten–platinum species,[2] we describe herein studies employing as a precursor the salt $[NEt_4][W(\equiv CC_6H_3Me_2\text{-}2,6)(CO)_2(\eta^5\text{-}C_2B_9H_9Me_2)]$ (**1b**). In this reagent the alkylidyne-carbon atom carries the bulky $C_6H_3Me_2$-2,6 substituent rather than the less sterically demanding C_6H_4Me-4 group. We have observed previously in studies[4] involving reactions between iron carbonyls and the compounds $[NEt_4][W(\equiv CR)(CO)_2(\eta^5\text{-}C_2B_9H_9Me_2)]$ (R = Me, Ph, C_6H_4Me-4, C_6H_4Me-2, or $C_6H_3Me_2$-2,6) that the products obtained depend on the nature of the substituent R. Use of alkylidyne–tungsten species containing the 2,6-dimethylphenyl or 2-methylphenyl groups leads to the identification of intermediates not seen with the less bulky aryl or alkyl fragments.[4]

Results and Discussion

Treatment of (**1b**) in acetone at −30 °C with two equivalents of $[PtH(Me_2CO)(PEt_3)_2][BF_4]$ afforded the compound $[WPtH(\mu\text{-}CC_6H_3Me_2\text{-}2,6)(CO)_2(PEt_3)(\eta^5\text{-}C_2B_9H_9Me_2)]$ (**4**) in *ca.* 60% yield. When equimolar amounts of the tungsten and platinum reagents are used in the synthesis of (**4**) the reaction

Table 2. Boron-11 and phosphorus-31 n.m.r. data[a] for the tungsten–platinum compounds

Compound	$^{11}B(\delta)^b$	$^{31}P(\delta)^c$
(4)	17.0 [1 B, B(μ-H)Pt] -9.1 to -19.8 (br 8 B)	^{d} 28.7 [J(PtP) 3 072]
(5a)	29.2 [1 B, BPt, J(PtB) 1 006] -3.5 to -16.4 (br, 8 B)	43.0 [J(PtP) 4 570, J(WP) 29]
(5b)	24.7 [1 B, BPt, J(PtB) 1 146], -2.9 (1 B), -3.8 (1 B), -7.3 (1 B), -11.3 (1 B), -13.6 (2 B), -15.0 (1 B), -20.7 (1 B)	43.4 [br, J(PtP) *ca.* 4 300]
(6a)	47.0 [1 B, BPt, J(PtB) 508], -7.9 to -15.0 (br, 8 B)	16.9 [J(PtP) 3 393]
(6b)	47.4 [1 B, BPt, J(PtB) 494] -8.1 to -23.3 (br, 8 B)	15.4 [J(PtP) 3 348]

[a] Chemical shifts (δ) in p.p.m., coupling constants in Hz, measurements at ambient temperatures in CD_2Cl_2–CH_2Cl_2 unless otherwise stated. [b] Hydrogen-1 decoupled, chemical shifts are positive to high frequency of $BF_3 \cdot Et_2O$ (external). [c] Hydrogen-1 decoupled, chemical shifts are positive to high frequency of 85% H_3PO_4 (external). [d] Measured in C_6D_6.

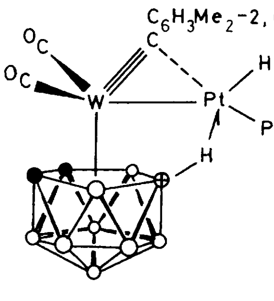

(4)

proceeds only half-way to completion. It was discovered that this was due to loss of platinum as the salt $[PtH(PEt_3)_3][BF_4]$, a species readily identified by the unique pattern of its hydrido resonance in the ^1H n.m.r. spectrum. The compound $[PtH(PEt_3)_3][BF_4]$ is produced by replacement of acetone in the reagent $[PtH(Me_2CO)(PEt_3)_2][BF_4]$ by PEt_3, the latter being released when the former combines with (**1b**).

Although, as described below, complex (**4**) slowly decomposes into other products, the spectroscopic data establish the structure. The i.r. spectrum revealed two absorptions at 1 998 and 1 931 cm^{-1} due to the carbonyl ligands. This is in contrast with the spectrum of (**2**)[2] which shows only one CO stretch at 1 828 cm^{-1}. The ^1H and ^{11}B-$\{^1H\}$ n.m.r. spectra (Tables 1 and 2) were especially informative. In the ^1H spectrum, in addition to the expected signals for the $C_6H_3Me_2$-2,6 and CMe groups, there is a very broad signal at δ −10.22 with strong ^{195}Pt–^1H coupling (1 165 Hz). This resonance is characteristic of a hydrido ligand terminally bound to platinum.[5] Moreover, the broadness of the peak suggested that the hydrido group is transoid to a boron nucleus. In addition, a very broad resonance occurs at δ −4.7, in the chemical shift range expected for a B–H⇀Pt group. Thus in the ^1H n.m.r. spectrum of the compound $[WPt(\mu\text{-}H)(CO)_2(PMe_3)(PEt_3)_2\{\eta^5\text{-}C_2B_9H_8(CH_2C_6H_4Me\text{-}4)Me_2\}][BF_4]$,[2] which also contains an exopolyhedral B–H⇀Pt fragment, the resonance for this moiety occurs at δ −5.4. The ^{11}B-$\{^1H\}$ n.m.r. spectrum of (**4**) confirms the presence of the B–H⇀Pt group. A resonance corresponding to one boron atom is seen at δ 17.0 p.p.m., the remaining eight boron nuclei giving rise to a broad signal in the range δ −9.1 to −19.8 p.p.m. Moreover, the signal at δ 17.0 p.p.m. shows ^1H–^{11}B coupling of *ca.* 45 Hz in the ^{11}B spectrum. Similar features are observed in the ^{11}B-$\{^1H\}$ and ^{11}B n.m.r. spectra of all species in which a $W(\eta^5\text{-}C_2B_9H_9Me_2)$ group is linked to a transition element both by a tungsten–metal bond and by an exopolyhedral B–H⇀metal interaction, the latter involving a BH group in the pentagonal face of the icosahedral η^5-$C_2B_9H_9Me_2$ ligand. In addition to the tungsten–platinum compounds mentioned above, structurally related dimetal complexes are known with W bonded to another W atom, or to Mo,[6a] Ru,[6b] or Ir[6c] atoms.

The ^{13}C-$\{^1H\}$ n.m.r. spectrum of (**4**) shows a signal at δ 277.2 p.p.m., appearing as a doublet due to ^{31}P–^{31}C coupling (29 Hz). This resonance is attributable to the alkylidyne-carbon nucleus, the coupling indicating a transoid arrangement of the μ-C–Pt–PEt_3 group. Interestingly, the observed chemical shift for the μ-C nucleus is not in the normal range for such resonances. Generally these signals are more deshielded (> 300 p.p.m.) when alkylidyne groups bridge two metal centres.[7] For example, in the tungsten–platinum compounds $[WPt(\mu\text{-}CC_6H_4Me\text{-}4)(CO)_2(PMe_2Ph)_2(\eta\text{-}C_5H_5)]$[8] and $[NEt_4][WPt(\mu\text{-}CPh)(CO)_2(cod)(\eta^5\text{-}C_2B_9H_9Me_2)]$[9] (cod = cyclo-octa-1,5-diene) the peaks in the ^{13}C-$\{^1H\}$ n.m.r. spectra for the μ-C groups appear at 336 and 312.8 p.p.m., respectively. In the salt (**1b**) the resonance for the terminally bound $CC_6H_3Me_2$-2,6 nucleus occurs at δ 299.2 p.p.m.[4b] As discussed further below, the chemical shift observed for the μ-C nucleus in (**4**) suggests strongly that the alkylidyne ligand asymmetrically bridges the W–Pt bond, being closer to the tungsten atom.

As mentioned earlier, compound (**4**) slowly decomposes into other complexes, and this is accelerated by stirring solutions of the compound in Et_2O for several hours, or by subjecting samples of (**4**) to column chromatography. The new compounds obtained *via* (**4**) are $[WPt(\mu\text{-}CC_6H_3Me_2\text{-}2,6)(CO)_2(PEt_3)(\mu\text{-}\sigma{:}\eta^5\text{-}C_2B_9H_8Me_2)]$ (**5**, two isomers), and $[WPt(\mu\text{-}CC_6H_3Me_2\text{-}2,6)(CO)_3(PEt_3)(\mu\text{-}\sigma{:}\eta^5\text{-}C_2B_9H_8Me_2)]$ (**6a**). Moreover, (**5**) and (**6a**) are formed with (**4**) if the initial reaction mixture obtained from (**1b**) and $[PtH(Me_2CO)(PEt_3)_2][BF_4]$ at −30 °C is allowed to warm to ambient temperatures before separation by chromatography.

The i.r. spectrum of (**6a**) shows three terminal CO stretching bands at 2 066m, 1 999vs, and 1 933s cm^{-1}, in accord with the presence of three carbonyl ligands. In contrast, the spectra of the two chromatographically separable isomers of (**5**) display two CO stretching bands [(**5a**), 1 996vs and 1 927s; (**5b**) 2 006vs and 1 930s cm^{-1}]. The n.m.r. data for the three species are summarised in Tables 1 and 2, but discussion is deferred until after the results of an *X*-ray diffraction study on (**5a**) have been described.

The molecular structure is shown in Figure 1, and the structural parameters are listed in Table 3. It is immediately apparent that (**5a**) is derived from (**4**) *via* loss of molecular hydrogen since the B–H⇀Pt link in the latter has been replaced by a B–Pt σ bond [2.01(2) Å] in the former. Moreover, there was no evidence of a terminal Pt–H group in (**5a**) either from the *X*-ray diffraction or ^1H n.m.r. data. The B(4)–Pt bond in (**5a**) is appreciably shorter than the B–Pt σ bond in (**3**) [2.123(5) Å].[2] A similar relationship holds for the W–Pt bonds [(**5a**), 2.728(1); (**3**), 2.843(2) Å]. The relatively shorter B–Pt and W–Pt distances in (**5a**) probably reflect unsaturation at the platinum centre (formally 14 electron) which is ligated by one PEt_3 group [Pt–P, 2.251(7) Å]. The tungsten atom carries two terminally bound CO groups and the η^5-$C_2B_9H_8Me_2$ cage. As a consequence of the B(4)–Pt interaction, the carbaborane group has undergone 'slippage' along the metal–metal bond accompanied by a folding of the C(1)C(2)B(3)B(4)B(5) face about B(3) and B(5). This leads to slip and fold parameters[10] of Δ 0.31 Å, θ 1.6°, and

Table 3. Selected internuclear distances (Å) and angles (°) for [$WPt(\mu\text{-}CC_6H_3Me_2\text{-}2,6)(CO)_2(PEt_3)(\mu\text{-}\sigma{:}\eta^5\text{-}C_2B_9H_8Me_2)$] (**5a**) and [$WPt(\mu\text{-}CC_6H_3Me_2\text{-}2,6)(CO)_3(PEt_3)(\mu\text{-}\sigma{:}\eta^5\text{-}C_2B_9H_8Me_2)$] (**6a**)

	(5a)	(6a)		(5a)	(6a)
W-Pt	2.728(1)	2.728(1)	Pt-P	2.251(7)	2.294(3)
W-C(5)	1.93(2)	2.05(2)	W-C(6)	1.98(2)	1.99(2)
W-C(1)	2.51(2)	2.46(1)	W-C(2)	2.51(2)	2.47(1)
W-B(3)	2.39(2)	2.33(1)	W-B(4)	2.29(2)	2.29(1)
W-B(5)	2.36(3)	2.38(1)	Pt-B(4)	2.01(2)	2.16(1)
C(1)-C(3)	1.60(2)	1.58(2)	C(2)-C(4)	1.53(4)	1.48(2)
C(1)-C(2)	1.52(3)	1.66(2)	C(1)-B(5)	1.73(3)	1.74(2)
C(2)-B(3)	1.74(3)	1.71(2)	B(3)-B(4)	1.88(3)	1.83(2)
B(4)-B(5)	1.80(2)	1.81(2)	C(5)-O(5)	1.21(3)	1.13(2)
C(6)-O(6)	1.18(2)	1.15(2)	W-C(20)	1.88(2)	1.89(1)
C(20)-C(21)	1.46(2)	1.44(2)	Pt-C(20)	2.15(2)	2.29(1)
Pt ··· C(21)	2.69(2)		Pt-C(7)		1.93(1)
C(7)-O(7)		1.14(1)			
W-Pt-P	155.9(1)	138.5(1)	W-C(5)-O(5)	172(2)	173(1)
W-C(6)-O(6)	176(2)	176(1)	C(5)-W-C(6)	90.0(8)	91.9(6)
W-C(20)-C(21)	175(1)	160.0(8)	Pt-C(20)-C(21)	95(1)	119(1)
Pt-W-C(20)	51.8(5)	55.9(3)	W-Pt-C(20)	43.2(4)	43.2(3)
W-C(20)-Pt	85.0(6)	80.8(4)	P-Pt-C(20)	160.6(4)	178.3(3)
P-Pt-B(4)	100.6(6)	87.0(3)	W-Pt-B(4)	55.4(6)	54.2(3)
C(1)-B(5)-B(4)	104(2)	106(1)	B(3)-B(4)-B(5)	105(2)	105(1)
C(2)-B(3)-B(4)	104(1)	108(1)	C(1)-C(2)-B(3)	112(2)	109(1)
C(2)-C(1)-B(5)	116(1)	112(1)	Pt-C(7)-O(7)		174(1)
C(20)-Pt-C(7)		83.5(4)			

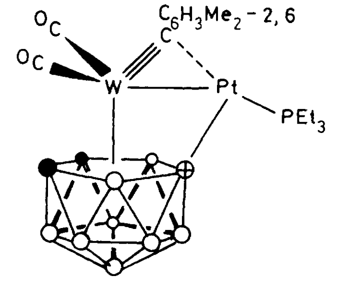

(5a)

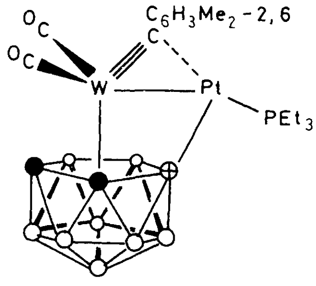

(5b)

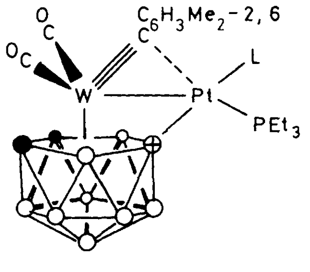

	L
(6a)	CO
(6b)	CNBu^t

φ 2.0°, which are substantially larger than those in compound (3).[2]

The bonding of the $CC_6H_3Me_2$-2,6 ligand in (**5a**) is of considerable interest. The W-C(20) bond length [1.88(2) Å] is little different from that for the W≡C linkage in the mononuclear tungsten compound [PPh_4][$W(\equiv CC_6H_4Me\text{-}4)(CO)_2(\eta^5\text{-}C_2B_9H_9Me_2)$] [1.826(7)Å].[9] Moreover, the W-C(20)-C(21) angle [175(1)°] corresponds to a nearly linear metal-alkylidyne group, which is disposed such as to place the plane defined by C(20)C(21)—C(28) at 87.4° to that defined by WPtC(20). The Pt-C(20) distance [2.15(2) Å] is significantly longer than the corresponding distance [1.997(9) Å]

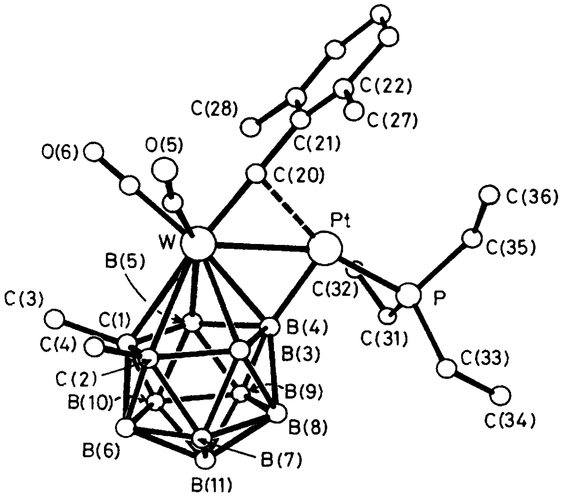

Figure 1. The molecular structure of $[WPt(\mu\text{-}CC_6H_3Me_2\text{-}2,6)(CO)_2(PEt_3)(\mu\text{-}\sigma{:}\eta^5\text{-}C_2B_9H_8Me_2)]$ (**5a**), showing the crystallographic numbering scheme

in the compound $[WPt(\mu\text{-}CC_6H_4Me\text{-}4)(CO)_2(PMe_2Ph)_2(\eta\text{-}C_5H_5)]$.[8] Moreover, in the latter the $W\text{-}\mu\text{-}C\text{-}C^1(C_6H_4Me\text{-}4)$ angle is 137.9(7)°. It is thus evident that in (**5a**) the alkylidyne ligand semi-bridges the W–Pt bond. Similar asymmetric alkylidyne ligand bonding is found in the two compounds $[WAu(\mu\text{-}CC_6H_4Me\text{-}4)(CO)_2(PPh_3)(\eta^5\text{-}C_2B_9H_9Me_2)]$[11] and $[WRu(\mu\text{-}CC_6H_4Me\text{-}4)(CO)_3(\eta\text{-}C_5H_5)(\eta^5\text{-}C_2B_9H_9Me_2)]$.[6b] However, the asymmetric bridging of the metal–metal bond by the alkylidyne group is more pronounced in (**5a**), since in the tungsten–gold and -ruthenium species the $W\text{-}\mu\text{-}C\text{-}C^1(C_6H_4\text{-}Me\text{-}4)$ angles are smaller, being 163(2) and 152.6(5)°, respectively.

Having established the structure of (**5a**) by *X*-ray diffraction, the n.m.r. data (Tables 1 and 2) are readily interpreted. The singlet in the $^{31}P\text{-}\{^1H\}$ n.m.r. spectrum at δ 43.0 p.p.m. shows very strong $^{195}Pt\text{-}^{31}P$ coupling (4 570 Hz), and also ^{183}W satellite peaks [J(WP) 29 Hz]. This is consistent with the transoid W–Pt–P (155.9°) arrangement. The $^{11}B\text{-}\{^1H\}$ n.m.r. spectrum reveals a resonance at δ 29.2 p.p.m., with J(PtB) 1 006 Hz. This peak may be assigned to the boron atom [B(4) in Figure 1] directly bonded to the platinum. As expected the resonance shows no $^1H\text{-}^{11}B$ coupling in the ^{11}B n.m.r. spectrum. The remaining eight boron nuclei give rise to broad signals in the range δ −3.5 to −16.4 p.p.m. In the $^{11}B\text{-}\{^1H\}$ n.m.r. spectrum of (**3**), which also contains a B–Pt exopolyhedral σ bond, the boron atom attached to platinum resonates at δ 36.2 p.p.m.[2] A $^{11}B\text{-}^{11}B$ two-dimensional COSY n.m.r. spectrum of (**5a**) confirmed that it is the central boron of the pentagonal $\overline{C\text{-}B\text{-}\mathit{B}\text{-}B\text{-}C}$ face which is bonded to the platinum, as found in the crystal (Figure 1). Only two cross peaks associated with the resonance at δ 29.2 p.p.m. were observed. This is as expected, since B(4) (Figure 1) lies in a plane of symmetry rendering the pairs of atoms B(3)B(5) and B(8)B(9) equivalent.

The ^1H n.m.r. spectrum of (**5a**) shows the characteristic peaks for the $C_6H_3Me_2$, Et, and CMe groups and no high-field signals, as found in the spectrum of the precursor (**4**). In the $^{13}C\text{-}\{^1H\}$ n.m.r. spectrum there is only one CO resonance in accord with the mirror plane of symmetry in the molecule. The resonance for the μ-C nucleus occurs at δ 279.9 p.p.m., as a doublet [J(PC) 22 Hz], with ^{183}W satellite peaks [J(WC) 146 Hz]. The chemical shift observed for the alkylidyne-carbon atom is as expected for the ligand semi-bridging the W–Pt bond. In the compounds $[WAu(\mu\text{-}CC_6H_4Me\text{-}4)(CO)_2(PPh_3)(\eta^5\text{-}C_2B_9H_9Me_2)]$[11] and $[WRu(\mu\text{-}CC_6H_4Me\text{-}4)(CO)_3(\eta\text{-}C_5H_5)(\eta^5\text{-}C_2B_9H_9Me_2)]$,[6b] which as discussed previously also contain semi-bridging alkylidyne groups, the $^{13}C\text{-}\{^1H\}$ n.m.r. peaks for the μ-C nuclei are at 292.9 and 276.7 p.p.m., respectively.

As mentioned earlier, in the synthesis of (**5a**) from (**4**), an isomer (**5b**) of the former species is produced in low yield (*ca.* 5%). The n.m.r. data (Tables 1 and 2) for (**5b**) establish the structure as one in which a boron atom adjacent to a CMe group in the pentagonal face of the cage is σ bonded to the platinum. As expected, the ^1H, $^{13}C\text{-}\{^1H\}$, $^{11}B\text{-}\{^1H\}$, and $^{31}P\text{-}\{^1H\}$ n.m.r. spectra of (**5a**) and (**5b**) are very similar. However, the absence of a mirror plane of symmetry in (**5b**) leads to the observation of two CO resonances (δ 221.2 and 218.6 p.p.m.) in the $^{13}C\text{-}\{^1H\}$ n.m.r. spectrum. A $^{11}B\text{-}^{11}B$ two-dimensional COSY n.m.r. spectrum revealed that there were three cross peaks associated with the resonance for the BPt group at δ 24.7 p.p.m. (Table 2). This is as anticipated for the structure proposed.

It is reasonable to assume that (**5b**) would form *via* the intermediacy of an isomer of (**4**) in which the $B\text{-}H\rightharpoonup Pt$ fragment employs a boron atom adjacent to a CMe group [see Scheme, intermediate (**A**)]. No spectroscopic evidence was obtained for this species, perhaps because it is less stable than (**4**), or it readily yields (**5b**), *via* loss of molecular hydrogen. As described earlier, loss of hydrogen from (**4**) affords the dominant product (**5a**), and it is possible that these processes proceed *via* reductive elimination from the dihydridoplatinum species (**B**) and (**C**).

Interestingly, the formation of (**5a**) from (**4**) can be reversed. If C_6D_6 solutions of the former are treated with a stream of hydrogen gas the latter is formed in *ca.* 10% yield, as deduced from ^1H and $^{11}B\text{-}\{^1H\}$ n.m.r. measurements. The interconversion of (**4**) and (**5**) represents, as far as we are aware, the first example of reversible oxidative-addition and reductive-elimination of a B–H group at a dimetal centre. In contrast with the reaction of (**5a**) with hydrogen, no reaction occurs with MeI or $SiHPh_3$, perhaps due to the steric requirements imposed by the $CC_6H_3Me_2\text{-}2,6$ group which shields the platinum centre.

When $[PtD(Me_2CO)(PEt_3)_2][BF_4]$ was used in the synthesis of (**4**), examination of the ^2H n.m.r. spectrum of the product revealed resonances at δ −10.0 and −4.7 due to Pt–D and $B\text{-}D\rightharpoonup Pt$ groups, respectively. In addition, there was a very broad signal at δ 2.6 attributable to terminal B–D groups. Exchange of D for H in the pentagonal face of the $\eta^5\text{-}C_2B_9H_9Me_2$ ligand can readily be accounted for (see Scheme) by the equilibria (**4**) $\rightleftharpoons$ (**A**) $\rightleftharpoons$ (**C**) and (**4**) $\rightleftharpoons$ (**B**). It should be noted that the former process requires rotation of the cage about an axis through the tungsten and the midpoint of the $\eta^5\text{-}\overline{B\text{-}B\text{-}B\text{-}C\text{-}C}$ ring. Similar behaviour has been observed with W–Ir complexes,[6c] and could involve an intermediate in which the $W(\eta^5\text{-}C_2B_9H_9Me_2)$ fragment does not partake in $B\text{-}H\rightharpoonup M$ (Pt or Ir) bonding, *i.e.* the $B\text{-}H\rightharpoonup Pt$ bond is lifted for rotation to occur.

The resonance at δ 2.6 in the deuteriated version of (**4**) is so broad and intense as to suggest that $^1H\text{-}^2H$ exchange has occurred with BH groups throughout the carbaborane cage. As mentioned earlier, $[PtH(PEt_3)_3][BF_4]$ is a reaction product. However, no exchange of deuterium for hydrogen was observed when $[PtD(PEt_3)_3][BF_4]$ was added to a non-deuteriated sample of (**4**), and this would seem to eliminate a bimolecular mechanism involving the former species for what is evidently a complicated process.

It was found that (**5a**) slowly isomerises to (**5b**) in solution. Likewise pure samples of (**5b**) afford (**5a**). Since these rearrangements do not require the presence of hydrogen they evidently do not proceed *via* (**4**) and (**A**) (see Scheme).A possible alternative route might be *via* the intermediates (**D**), (**E**), and (**F**), the formation of which might be facilitated by the Pt centre in (**5a**)

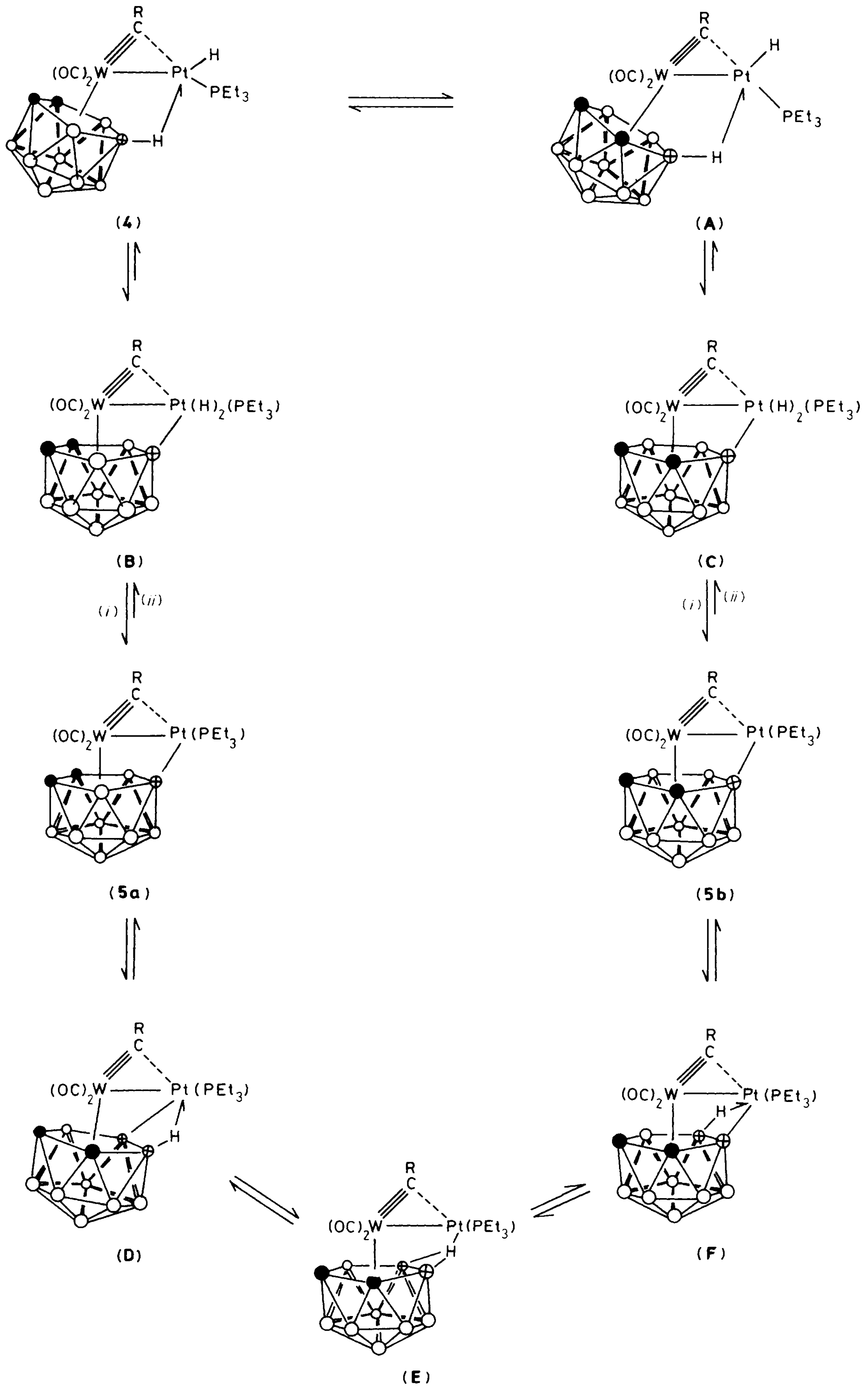

Scheme. R = $C_6H_3Me_2$-2,6; ○ = BH, ● = CMe, ⊕ = B; (*i*) $-H_2$, (*ii*) $+ H_2$

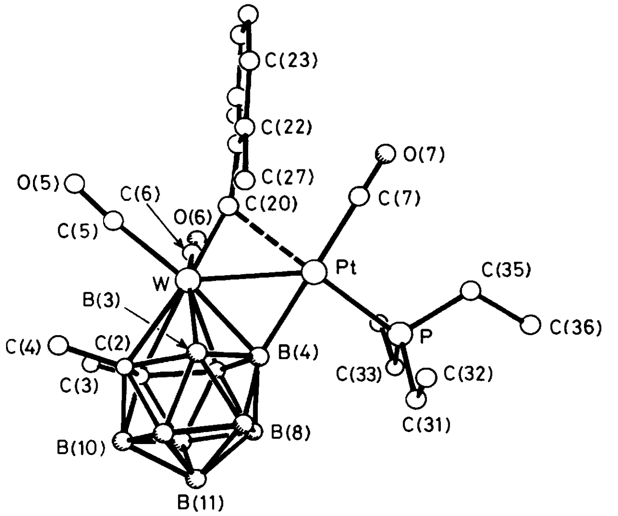

Figure 2. The molecular structure of $[WPt(\mu\text{-}CC_6H_3Me_2\text{-}2,6)(CO)_3(PEt_3)(\mu\text{-}\sigma{:}\eta^5\text{-}C_2B_9H_8Me_2)]$ (**6a**), showing the crystallographic numbering scheme

and (**5b**) being formally in a 14-electron environment. This could promote formation of the B–H⇀Pt three-centre two-electron bonds in (**D**) and (**F**), and allow these two species to equilibrate *via* (**E**) having a μ_3-H group.

Treatment of solutions of (**5a**) with CO affords compound (**6a**) quantitatively. As mentioned earlier, (**6a**) is also formed as a by-product in the preparation of (**5a**), and this is evidently due to the latter scavenging CO from species present in the mixtures.

The molecular structure of (**6a**) was established by an *X*-ray diffraction study, and the molecule is shown in Figure 2. Structural parameters are listed in Table 3 alongside those of compound (**5a**), since the data for the two species are very similar. The presence of the terminal PtCO group in (**6a**) leads to a reduction in the W–Pt–P angle [138.5(1)°] compared with that in (**5a**) [155.9(1)°]. Moreover, the W–μ-C–$C^1(C_6H_3)$ angle in (**6a**) [160.0(8)°] is somewhat less than that in (**5a**) [175(1)°]. In (**6a**), as in (**5a**), it is the central boron atom of the $\overline{\text{C–C–B–}\textit{B}\text{–B}}$ pentagonal face of the carbaborane ligand which is σ bonded to the platinum. The presence of the PtCO group in (**6a**) leads to a longer B–Pt σ bond [2.16(1) Å] compared with (**5a**) [2.01(2) Å].

The n.m.r. data (Tables 1 and 2) for (**6a**) are in accord with the structure established by *X*-ray diffraction, and call for little comment. The chemical shift (δ 287.9 p.p.m.) for the μ-C group in the $^{13}C\text{-}\{^1H\}$ n.m.r. spectrum correlates with the asymmetric bridging of the W–Pt bond by this ligand, as discussed above for (**5a**).

In contrast with the reaction of (**5a**) with CO, reactions with tertiary phosphines led to decomposition. However, the rod-like ligand CNBu^t, which is less sterically demanding, readily combined with (**5a**) to give the complex $[WPt(\mu\text{-}CC_6H_3Me_2\text{-}2,6)(CO)_2(CNBu^t)(PEt_3)(\mu\text{-}\sigma{:}\eta^5\text{-}C_2B_9H_8Me_2)]$ (**6b**). The spectroscopic and analytical data for (**6b**) establish that it is structurally similar to (**6a**). The i.r. spectrum shows a band for the NC group at 2 178 cm^{-1}, and two CO stretches at 1 988 and 1 919 cm^{-1}. The $^{13}C\text{-}\{^1H\}$ n.m.r. spectrum (Table 1) shows the characteristic resonance for the μ-C nucleus at δ 291.7 p.p.m., which appears as a doublet due to $^{31}P\text{–}^{13}C$ coupling (38 Hz) with the transoid PEt_3 ligand. The resonance for the ligated *C*NBu^t nucleus is seen at δ 127.3 p.p.m. The $^{31}P\text{-}\{^1H\}$ and $^{11}B\text{-}\{^1H\}$ spectra (Table 2) are very similar to those of (**6a**). In particular, the $^{11}B\text{-}\{^1H\}$ n.m.r. spectrum of (**6b**) shows a diagnostic peak for the BPt group at δ 47.4 p.p.m., an assignment confirmed by the appearance of $^{195}Pt\text{–}^{11}B$ satellite peaks corresponding to a coupling of 494 Hz.

The results described in this paper represent a striking contrast with those described earlier[2] which led to the synthesis of compound (**2**). The presence of the bulky $C_6H_3Me_2$-2,6 group in (**1b**) results in the observation of a very different reactivity pattern to that found with (**1a**). This difference has also been found recently in reactions of the anionic complexes $[W(\equiv CR)(CO)_2(\eta^5\text{-}C_2B_9H_9Me_2)]^-$ with iron carbonyls.[4b] As mentioned in the Introduction, the formation of (**2**) probably proceeds *via* an intermediate in which a μ-$CH(C_6H_4Me\text{-}4)$ group, formed by hydride transfer from platinum to a μ-alkylidyne ligand, inserts into a B–H moiety activated by B–H⇀Pt bonding.[2] A similar process involving (**1b**) and $[PtH(Me_2CO)(PEt_3)_2][BF_4]$ may be sterically inhibited leading instead to loss of hydrogen, as compound (**4**) affords (**5**) rather than a product akin to (**2**).

Experimental

All experiments were carried out using Schlenk-tube techniques under a dry oxygen-free nitrogen atmosphere. Light petroleum refers to that fraction of b.p. 40—60 °C. The salts $[NEt_4][W(\equiv CC_6H_3Me_2\text{-}2,6)(CO)_2(\eta^5\text{-}C_2B_9H_9Me_2)]$[4b] and $[PtH(Me_2CO)(PEt_3)_2][BF_4]$[12] were prepared as described earlier. Products were separated by column (3 × 30 cm) chromatography on Florisil (Aldrich, 100—200 mesh). The instrumentation employed for spectroscopic measurements has been reported in previous parts of this series.[4,6]

Reactions between $[NEt_4][W(\equiv CC_6H_3Me_2\text{-}2,6)(CO)_2(\eta^5\text{-}C_2B_9H_9Me_2)]$ *and* $[PtH(Me_2CO)(PEt_3)_2][BF_4]$.—(*i*) The compound *trans*-$[PtH(Cl)(PEt_3)_2]$ (0.30 g, 0.63 mmol) in acetone (10 cm^3) was treated with $AgBF_4$ (0.14 g, 0.70 mmol) to generate $[PtH(Me_2CO)(PEt_3)_2][BF_4]$ and AgCl. The solution containing the former was decanted through a Celite pad (2 × 2 cm) into a cold (*ca.* −30 °C) stirred acetone (10 cm^3) solution of (**1b**) (0.21 g, 0.32 mmol). The AgCl residue was treated with additional acetone (10 cm^3) and the washings were passed through the Celite pad into the reaction mixture. The latter changed colour from orange to red, and after 45 min the solvent was removed at −30 °C (*ca.* 2 h) *in vacuo.* The residue was extracted with cold Et_2O (−70 °C, 2 × 20 cm^3) and the extracts were chromatographed at the same temperature. Elution with Et_2O afforded a red eluate which after removal of solvent *in vacuo* gave red *microcrystals* of $[WPtH(\mu\text{-}CC_6H_3Me_2\text{-}2,6)(CO)_2(PEt_3)(\eta^5\text{-}C_2B_9H_9Me_2)]$ (**4**) (0.16 g) [$\nu_{max.}$(BH) at 2 565w,br, $\nu_{max.}$(CO) at 1 998vs and 1 931s cm^{-1}] of *ca.* 80% purity as deduced from spectroscopic data (see Results and Discussion section). Further chromatography of (**4**) led to more extensive conversion into (**5**).

(*ii*) The reaction between (**1b**) (0.76 g, 1.17 mmol) and $[PtH(Me_2CO)(PEt_3)_2][BF_4]$ (2.34 mmol) was carried out as described above but after 45 min the mixture was warmed to room temperature before the acetone solvent was removed *in vacuo.* The residue was dissolved in Et_2O (30 cm^3) and stirred for 36 h, after which period the solution was reduced in volume *in vacuo* to *ca.* 15 cm^3 and the same volume of light petroleum added. The mixture was then chromatographed (−30 °C), three bands developing on the column. Elution with the same solvent mixture, followed by removal of solvent, afforded initially pink *microcrystals* of $[WPt(\mu\text{-}CC_6H_3Me_2\text{-}2,6)(CO)_3(PEt_3)(\mu\text{-}\sigma{:}\eta^5\text{-}C_2B_9H_8Me_2)]$ (**6a**) (0.19 g, 19%) (Found: C, 31.1; H, 4.8. $C_{22}H_{38}B_9O_3PPtW$ requires C, 30.8; H, 4.5%); $\nu_{max.}$(CO) at 2 066m, 1 999vs, and 1 933s cm^{-1} (Et_2O), followed by red *microcrystals* of $[WPt(\mu\text{-}CC_6H_3Me_2\text{-}2,6)(CO)_2(PEt_3)(\mu\text{-}\sigma{:}\eta^5\text{-}C_2B_9H_8Me_2)]$ (**5a**) (0.24 g, 25%) (Found: C, 30.5; H, 5.1. $C_{21}H_{38}B_9O_2PPtW$ requires C, 30.4; H, 4.6%); $\nu_{max.}$(CO) at 1 996vs and 1 927s cm^{-1} (Et_2O).

Table 4. Atomic positional parameters (fractional co-ordinates, × 10^4) for complex (**5a**), with estimated standard deviations in parentheses

Atom	x	y	z
W	6 523(1)	4 316(1)	2 945(1)
Pt	7 954(1)	5 278(1)	2 778(1)
P	9 312(4)	5 403(4)	2 660(4)
C(5)	6 195(13)	4 651(14)	3 949(12)
O(5)	6 025(12)	4 979(11)	4 566(10)
C(6)	5 170(13)	4 475(13)	1 970(14)
O(6)	4 382(10)	4 596(11)	1 347(11)
C(1)	6 424(11)	2 481(12)	2619(12)
C(2)	6 925(12)	2 620(11)	3 703(13)
C(3)	5 322(13)	2 180(15)	2 055(16)
C(4)	6 413(15)	2 455(14)	4 309(14)
B(3)	7 895(14)	3 419(14)	4 082(14)
B(4)	7 893(11)	3 797(12)	2 928(11)
B(5)	6 866(15)	3 186(12)	1 997(17)
B(6)	7 104(18)	1 501(16)	3 225(16)
B(7)	8 131(19)	2 079(18)	4 189(20)
B(8)	8 713(17)	2 865(16)	3 698(18)
B(9)	8 057(14)	2 690(14)	2 394(17)
B(10)	7 097(16)	1 874(14)	2 153(16)
B(11)	8 213(17)	1 671(15)	3 175(19)
C(20)	6 625(10)	5 677(11)	2 750(10)
C(21)	6 669(10)	6 716(10)	2 506(11)
C(22)	7 039(12)	7 366(12)	3 252(14)
C(23)	7 116(16)	8 404(13)	3 006(18)
C(24)	6 738(18)	8 754(16)	2 100(19)
C(25)	6 360(15)	8 018(15)	1 398(16)
C(26)	6 281(11)	7 035(12)	1 550(12)
C(27)	7 456(17)	7 079(14)	4 338(13)
C(28)	5 837(15)	6 311(15)	716(14)
C(31)	9 187(17)	4 936(18)	1 537(17)
C(32)	8 306(25)	5 294(19)	689(19)
C(33)	10 368(15)	4 767(19)	3 585(18)
C(34)	11 255(16)	4 859(21)	3 532(18)
C(35)	9 615(26)	6 708(21)	2 665(30)
C(36)	9 483(27)	7 339(23)	3 218(37)

Table 5. Atomic positional parameters (fractional co-ordinates, × 10^4) for complex (**6a**), with estimated standard deviations in parentheses

Atom	x	y	z
Pt	1 542(1)	3 859(1)	2 417(1)
W	−664(1)	2 644(1)	3 118(1)
P	2 057(3)	4 852(4)	1 295(1)
C(1)	−2 900(12)	2 182(16)	2 471(7)
C(2)	−2 466(11)	342(19)	2 547(6)
C(3)	−3 890(15)	2 716(24)	2 966(9)
C(4)	−3 040(16)	−853(19)	3 102(10)
C(5)	−964(14)	1 491(18)	4 095(8)
O(5)	−1 040(12)	1 002(17)	4 666(6)
C(6)	−745(14)	4 876(18)	3 532(7)
O(6)	−786(12)	6 198(13)	3 730(6)
C(7)	3 267(11)	4 863(15)	2 903(6)
O(7)	4 249(10)	5 579(16)	3 191(5)
C(20)	1 094(11)	2 882(14)	3 549(5)
C(21)	2 177(11)	2 748(15)	4 068(5)
C(22)	2 761(12)	1 386(16)	4 031(7)
C(23)	3 721(13)	1 158(19)	4 560(8)
C(24)	4 151(14)	2 345(21)	5 127(7)
C(25)	3 583(12)	3 703(18)	5 177(6)
C(26)	2 623(12)	3 948(16)	4 649(6)
C(27)	2 290(17)	48(18)	3 421(9)
C(28)	2 082(15)	5 523(20)	4 662(8)
C(31)	1 746(13)	3 348(16)	530(6)
C(32)	2 454(18)	1 920(18)	675(9)
C(33)	1 221(13)	6 495(16)	1 030(7)
C(34)	1 371(23)	7 812(23)	1 632(11)
C(35)	3 832(10)	5 751(15)	1 299(5)
C(36)	4 315(17)	6 607(24)	604(8)
B(3)	−954(12)	527(18)	2 228(8)
B(4)	−412(12)	2 688(14)	1 904(6)
B(5)	−1 714(13)	3 720(17)	2 087(7)
B(6)	−2 425(15)	−407(19)	1 641(8)
B(7)	−1 193(14)	986(19)	1 293(7)
B(8)	−1 653(14)	2 905(18)	1 205(7)
B(9)	−3 196(15)	2 663(23)	1 553(9)
B(10)	−3 685(15)	604(23)	1 854(9)
B(11)	−2 884(15)	965(20)	1 051(8)

Elution of the chromatography column with Et_2O removed a slow moving fraction which yielded after removal of solvent red *microcrystals* of $[WPt(\mu\text{-}CC_6H_3Me_2\text{-}2,6)(CO)_2(PEt_3)(\mu\text{-}\sigma{:}\eta^5\text{-}C_2B_9H_8Me_2)]$ (**5b**) (0.05 g, 5%) (Found: C, 29.7; H, 5.1. $C_{21}H_{38}B_9O_2PPtW$ requires C, 30.4; H, 4.6%); $\nu_{max.}$(CO) at 2 006vs and 1 930s cm^{-1} (Et_2O).

An analytically pure sample of (**5a**) was obtained only after twice re-chromatographing the initially obtained product. Each chromatographic separation gave an additional trace of (**5b**).

Reactions of $[WPt(\mu\text{-}CC_6H_3Me_2\text{-}2,6)(CO)_2(PEt_3)(\mu\text{-}\sigma{:}\eta^5\text{-}C_2B_9H_8Me_2)]$ (**5a**).—(*i*) Carbon monoxide was bubbled through an Et_2O (20 cm^3) solution of (**5a**) (0.25 g, 0.30 mmol) for 1 min, producing a colour change from red to pale purple. Removal of solvent *in vacuo* afforded quantitatively pink *microcrystals* of (**6a**).

(*ii*) An Et_2O (5 cm^3) solution of (**5a**) (0.05 g, 0.06 mmol) was treated with $CNBu^t$ (0.06 mmol; 0.05 cm^3 of a 1.2 mol dm^{-3} solution in Et_2O), and the mixture was stirred for 15 min. Removal of solvent *in vacuo* gave red *microcrystals* of $[WPt(\mu\text{-}CC_6H_3Me_2\text{-}2,6)(CO)_2(CNBu^t)(PEt_3)(\mu\text{-}\sigma{:}\eta^5\text{-}C_2B_9H_8Me_2)]$ (**6b**) (0.05 g, 90%) (Found: C, 34.1; H, 5.4; N, 1.8. $C_{26}H_{47}B_9NO_2PPtW$ requires C, 34.2; H, 5.2; N, 1.5%); $\nu_{max.}$(in Et_2O) at 2 178m (NC), 1 988vs and 1 919s cm^{-1} (CO). Analytically pure samples of (**6b**) were obtained by chromatography at −30 °C, eluting with Et_2O.

(*iii*) Hydrogen gas was bubbled for 1 min through an n.m.r. tube containing a C_6D_6 (0.6 cm^3) solution of pure (**5a**) (0.05 mmol). The n.m.r. spectra (^1H and $^{11}B\text{-}\{^1H\}$) were recorded, and relative peak intensities in the spectra indicated the presence of *ca.* 10% of (**4**).

Crystal Structure Determinations.—Crystals of the dimetal compounds (**5a**) and (**6a**) grow as red prisms and red rhomboids, respectively, from light petroleum at −20 °C. Crystals for study [(**5a**), *ca.* 0.8 × 0.5 × 0.5 mm; (**6a**), *ca.* 0.7 × 0.3 × 0.2 mm diameter cut from a larger crystal] were sealed in Lindemann glass capillaries under dry nitrogen. Diffracted intensities were collected [(**5a**), Wyckoff ω scans; (**6a**) θ–2θ scan mode] on a Nicolet *P*3*m* diffractometer at 298 K, in the range $2.9 \leqslant 2\theta \leqslant 50°$. For (**5a**) of 5 740 intensities, 3 455 unique data had $F \geqslant 5\sigma(F)$, and only these were used in the final refinement of the structure, after all the data had been corrected for Lorentz and polarisation effects and an empirical correction applied for *X*-ray absorption.[13] Correspondingly for (**6a**), of 5 988 reflections, 4 791 had $F \geqslant 3\sigma(F)$, and only these were used in refinement, after similar corrections had been applied.

Crystal data for (**5a**). $C_{21}H_{38}B_9O_2PPtW$, $M = 829.75$, monoclinic, $a = 15.845(11)$, $b = 13.454(6)$, $c = 15.725(12)$ Å, $\beta = 117.98(5)°$, $U = 2\,960(3)$ Å^3, $D_c = 1.86$ g cm^{-3}, $Z = 4$, $F(000) = 1\,568$, space group $P2_1/c$ (no. 14), Mo-K_α *X*-radiation (graphite monochromator), $\bar{\lambda} = 0.710\,69$ Å, $\mu(\text{Mo-}K_\alpha) = 88.9$ cm^{-1}.

Crystal data for (**6a**). $C_{22}H_{38}B_9O_3PPtW$, $M = 857.8$, triclinic, $a = 10.416(10)$, $b = 8.133(3)$, $c = 18.508(15)$ Å, $\alpha = 89.91(5)$, $\beta = 95.46(7)$, $\gamma = 103.52(6)^\circ$, $U = 1\,517(2)$ Å^3, $D_c = 1.88$ g cm^{-3}, $Z = 2$, $F(000) = 812$, space group $P\bar{1}$, $\mu(\text{Mo-}K_\alpha) = 86.0$ cm^{-1}.

Structure solutions and refinement. The structures were solved by heavy-atom methods, and all non-hydrogen atoms were located by difference-Fourier calculations. All refinements involved blocked-cascade techniques. For (**5a**) anisotropic thermal parameters were used for all non-hydrogen atoms with the exception of B(4) and C(20). Attempts to refine these atoms with anisotropic thermal parameters were unsuccessful, presumably reflecting relatively poor quality of the data since the crystal diffracted poorly revealing comparatively broad and asymmetric intensity distributions. Hydrogen atoms were not included in the refinement of (**5a**). However, for (**6a**) C–H (0.96 Å) and B–H (1.10 Å) hydrogen atoms were included with fixed isotropic thermal parameters (*ca.* 1.2 × U_{equiv} of the carbon and boron atom to which they were attached). Refinement led to $R = 0.056$ ($R' = 0.058$) for (**5a**), and $R = 0.062$ ($R' = 0.059$) for (**6a**). Weighting schemes of the form $w^{-1} = [\sigma^2(F_o) + g|F_o|^2]^{-1}$ where $g = 0.001$ for (**5a**) and 0.0008 for (**6a**) gave a satisfactory analysis of variance. The final electron-density difference synthesis showed no peaks < or > 1.0 e Å^{-3} for (**5a**). For (**6a**) peaks of *ca.* 4.7 e Å^{-3} were found in the vicinity of the metal atoms which presumably reflects our inability adequately to correct for absorption in this structure. Scattering factors with corrections for anomalous dispersion were taken from ref. 14. All calculations were carried out with the SHELXTL system of programs.[13] Atomic co-ordinates are given in Tables 4 and 5.

Additional material available from the Cambridge Crystallographic Data Centre comprises H-atom co-ordinates, thermal parameters, and remaining bond lengths and angles.

Acknowledgements

We thank the S.E.R.C. for a research studentship (to M. U. P.) and the U.S. Air Force Office of Scientific Research (Grant 86-0125) for partial support.

References

1 Part 83, J. R. Fernández and F. G. A. Stone, *J. Chem. Soc., Dalton Trans.*, 1988, 3035.

2 M. J. Attfield, J. A. K. Howard, A. N. de M. Jelfs, C. M. Nunn, and F. G. A. Stone, *J. Chem. Soc., Dalton Trans.*, 1987, 2219.

3 J. D. Kennedy, *Inorg. Chem.*, 1986, **25**, 111; R. T. Baker, *ibid.*, p. 109; R. L. Johnston, and D. M. P. Mingos, *ibid.*, p. 3391.

4 (*a*) F-E. Baumann, J. A. K. Howard, O. Johnson, and F. G. A. Stone, *J. Chem. Soc., Dalton Trans.*, 1987, 2917; (*b*) F-E. Baumann, J. A. K. Howard, R. J. Musgrove. P. Sherwood, and F. G. A. Stone, *ibid.*, 1988, 1879.

5 D. M. Roundhill, *Adv. Organomet. Chem.*, 1975, **13**, 273; H. D. Kaesz and R. B. Saillant, *Chem. Rev.*, 1972, **72**, 231.

6 (*a*) M. Green, J. A. K. Howard, A. P. James, A. N. de M. Jelfs, C. M. Nunn, and F. G. A. Stone, *J. Chem. Soc., Dalton Trans.*, 1987, 81, 1221; (*b*) M. Green, J. A. K. Howard, A. N. de M. Jelfs, O. Johnson, and F. G. A. Stone, *ibid.*, p. 73; (*c*) F-E. Baumann, J. A. K. Howard, R. J. Musgrove, P. Sherwood, M. A. Ruiz, and F. G. A. Stone, *J. Chem. Soc., Chem. Commun.*, 1987, 1881.

7 J. A. Abad, L. W. Bateman, J. C. Jeffery, K. A. Mead, H. Razay, F. G. A. Stone, and P. Woodward, *J. Chem. Soc., Dalton Trans.*, 1983, 2075; M. Green, J. A. K. Howard, A. P. James, A. N. de M. Jelfs, C. M. Nunn, and F. G. A. Stone, *ibid.*, 1986, 1697.

8 T. V. Ashworth, J. A. K. Howard, and F. G. A. Stone, *J. Chem. Soc., Dalton Trans.*, 1980, 1609.

9 F-E. Baumann, J. A. K. Howard, O. Johnson, and F. G. A. Stone, *J. Chem. Soc., Dalton Trans.*, 1987, 2661; O. Johnson and J. A. K. Howard, *ibid.*, 1988, 2903.

10 D. M. P. Mingos, M. I. Forsyth, and A. J. Welch, *J. Chem. Soc., Dalton Trans.*, 1978, 1363.

11 M. Green, J. A. K. Howard, A. P. James, C. M. Nunn, and F. G. A. Stone, *J. Chem. Soc., Dalton Trans.*, 1987, 61.

12 D. Afzal. P. G. Lenhert, and C. M. Lukehart, *J. Am. Chem. Soc.*, 1984, **106**, 3050.

13 G. M. Sheldrick, SHELXTL programs for use with the Nicolet *X*-ray system, Cambridge, 1976; updated Göttingen, 1981.

14 'International Tables for *X*-Ray Crystallography,' Kynoch Press, Birmingham, 1974, vol. 4.

Received 26*th April* 1988; *Paper* 8/01631C